$JU - 71$

46311

$P_ 12$

Supersonic Coaxial Jet Noise Predictions

Milo D. Dahl
Lewis Research Center
Cleveland, Ohio

and

Philip J. Morris
Pennsylvania State University
University Park, Pennsylvania

National Aeronautics and
Space Administration

(NASA-TM-106917)   SUPERSONIC
COAXIAL JET NOISE PREDICTIONS
(NASA. Lewis Research Center)   12 p

N95-26801

Unclas

G3**/71   0048311

SUPERSONIC COAXIAL JET NOISE PREDICTIONS

Milo D. Dahl*
NASA Lewis Research Center
Cleveland, OH 44135

Philip J. Morris†
Penn State University
University Park, PA 16802

ABSTRACT

Predictions are made for the noise radiation from supersonic, coaxial jets. These predictions are based on the assumption that the noise radiation in the downstream direction of supersonic jets is dominated by sound generated by instability waves with supersonic phase velocities relative to ambient. Since the analysis requires a known mean flow and the coaxial jet mean flow is not described easily in terms of analytic functions, a numerical prediction is made for its development. The compressible, Reynolds averaged, boundary layer equations are solved with a modified mixing length turbulence model. The model has been calibrated to account for compressibility and temperature effects on the rate of mixing. Both normal and inverted velocity profile jets are considered. Predictions are made for the differences between the noise radiated by coaxial jets with different operating conditions and a single reference jet with the same thrust, mass flow, and exit area. The effects of area ratio changes and simulated enhanced mixing on noise radiation are also considered.

1 INTRODUCTION

Supersonic jets are intense noise generators and means must be found to modify the noise generation process to reduce radiated noise levels if a future high speed civilian aircraft is to meet community noise regulations. In a recent review, Seiner and Krejsa[1] discuss the challenge of reducing supersonic jet noise associated with both mixing and shocks while maintaining acceptable propulsion system performance requirements. In this paper, we examine a method to modify the noise generation from a supersonic jet by replacing the single stream jet with a dual stream, coaxial jet. The total thrust and mass flow are maintained when using the dual stream jet and the interaction between the two shear layers is used to reduce the strength of the noise sources. When the coaxial jet flow has a higher inner stream velocity than an outer stream velocity, it is referred to as a normal velocity profile (NVP) jet. If the outer stream velocity is

higher than the inner stream velocity, the jet has an inverted velocity profile (IVP). For supersonic, perfectly expanded jets, instability waves or large scale coherent structures dynamically control the development of free jet shear flows. When the instability wave phase velocities exceed the ambient speed of sound, these waves are the dominant source of mixing noise radiated into the downstream arc of the jet. This instability wave noise generation model, previously applied to single stream jets, is extended here to dual stream, coaxial jets and is the basis for the results presented in this paper.

Interest in the noise radiated from coaxial jets increased with the introduction of the by-pass jet engine. Noise measurements from these subsonic NVP coaxial jets led to the consensus that they were quieter due to lower velocities at the same mass flow compared to single jets. When the coaxial jets were operated with supersonic conditions, the primary concern became the reduction of shock noise (Yu and Dosanjh[2]). Compared to a single stream, shock containing jet, operating conditions were found for the coaxial jet that minimized the shock noise and thus the overall radiated noise levels. Tanna et al.[3] conducted a systematic study of shock containing coaxial jets using fixed thrust, mass flow, and exit area conditions and obtained similar results for minimum shock noise conditions. When these systematic conditions were applied to lower speed, shock free IVP[4] and NVP[5] jets, the NVP jets were always noisier than the single reference jet while the IVP jets could have noise reductions. This type of noise result was also seen in shock containing coaxial jets operated at minimum shock noise conditions.

When the supersonic jet is perfectly expanded, the instability waves generate noise that has a radiation pattern with a dominant peak in the downstream arc of the jet. Even when shocks are present in the jet flow, the noise from the jet that radiates into the downstream arc is due primarily to mixing; whereas, the broadband shock associated noise dominates in the upstream arc. Extensive measurements have shown this for single jets[6] and for coaxial jets.[7] In a previous study, Dahl and Morris[8] developed a prediction scheme that could analyze the mixing noise, where it dominates, from supersonic coaxial jets. Assuming the jet to be perfectly expanded simplified the analysis and allowed the study to concentrate on exit velocity profile shaping as a means to

1

further reduce the mixing noise. That study only considered a limited number of operating conditions and area ratios.

In this paper, we examine what happens to the predicted noise levels as the coaxial jet flow is modified. To generate the developing mean flow, a numerical prediction scheme was used and is described in the next section. This is followed by an outline of the calculations for the evolving instability waves and their noise radiation patterns. The results for different coaxial jet flows then follow. First for the NVP jets, the operating conditions are varied for a fixed area ratio and then, the jet exit area ratio is changed. This is followed by a similar set of calculations for the IVP jets. Finally, we examine what happens when the mixing rates in the jet shear layers are enhanced. This is achieved by modifying the mixing length coefficients in the turbulence model. In practice, this could be achieved by the addition of vortex generators or mixers at the jet exit.[9]

2 MEAN FLOW DEVELOPMENT

Analytic functions have been commonly used to characterize the mean flow profiles so that the calculations of instability waves in single axisymmetric jets can be completed. These analytic functions have been based on results from experimental measurements. The measured data typically include only velocity profile results which are sufficient for incompressible instability wave calculations. When compressibility is important, the instability wave calculations require that either the temperature or the density profile be specified. The approximation is then often made that the Crocco-Busemann relation applies. This defines the temperature or density profile to be a function of the velocity profile. Michalke[10] has summarized the use of analytic functions in the calculation of stability characteristics for both incompressible and compressible jets. To fully describe the axial growth and decay of the instability wave, the mean flow development must be described at all axial locations. In this case, Tam and Burton[11] let the parameters of the analytic function vary with axial location according to cubic spline fits to measured velocity profile data.

When it comes to supersonic coaxial jets, it is not clear how to derive appropriate analytic functions to describe the velocity profiles at all axial locations. There is little measured data for coaxial jets with supersonic conditions that would allow an analytical description to be made at all axial locations including the merging region of a normal profile and an inverted profile into a single jet. Furthermore, even though velocity measurements may be available for coaxial jets with supersonic conditions, it is doubtful that the Crocco-Busemann relation could provide the appropriate density profiles for either normal or inverted velocity profile conditions. Thus, the decision was made to generate mean profiles for coaxial jets numerically. Morris[12] and Morris and Baltas[13] calculated instability waves using numerically generated

velocity profiles for a single incompressible jet. The extension here is to include compressibility effects into the spreading and merging of a coaxial jet and generate both velocity and density profiles. As the basis for the numerical mean flow analysis, we use a set of compressible, Reynolds averaged, boundary layer equations with a modified mixing length model to determine the Reynolds stresses. The jet static pressure is matched to the ambient pressure; hence, the flow is perfectly expanded.

2.1 Turbulence Model

In the development of a prediction scheme for the mean flow properties of a coaxial jet, simplicity and robustness were emphasized in order to calculate the mean velocity and density and their derivatives accurately for later use in the instability wave calculations. This led us to choose a simple turbulence model, resulting in a high level of empiricism.

The compressible equations of motion are simplified to the boundary layer form. The assumption is also made that the density-velocity correlations may be neglected. For the single axisymmetric shear layer case, the Reynolds stress and the heat flux terms are described by the following mixing-length model:

$$ -\rho\overline{u'v'} = \mu_{\mathrm{T}}\frac{\partial u}{\partial r} \qquad (1) $$

and

$$ -\rho c_p\overline{v'T'} = \frac{c_p\mu_{\mathrm{T}}}{\mathrm{Pr_T}}\frac{\partial T}{\partial r} \qquad (2) $$

with

$$ \mu_{\mathrm{T}} = \rho\left(C_1 C_2 \ell\right)^2 \left|\frac{\partial u}{\partial r}\right|. \qquad (3) $$

ℓ is a characteristic mixing length scale given by

$$ \ell = \frac{\Delta U}{|\partial u/\partial r|_{\max}}. \qquad (4) $$

The factor C_1 is the incompressible part of the mixing length constant. It depends on the the velocity ratio U_2/U_1 and the density ratio ρ_2/ρ_1. The C_2 factor is the compressible part of the mixing length constant. Its purpose is to decrease the growth of the shear layer as compressibility effects become important. It depends on a Mach number in a frame of reference convecting with the real phase speed of a growing disturbance in the shear layer. This convected Mach number depends on the velocity ratio, the density ratio, and the Mach number of the jet. Thus, both factors depend on the flow conditions and a calibration procedure was developed to obtain empirical equations to describe both factors. The details are given in Dahl.[14]

Initially, a coaxial jet has two distinct shear layers with uniform flow conditions at both edges of both shear layers. As a result, the mixing length model, equation (3), gives separate constant values C_1, C_2, and ℓ

for each shear layer. This will at some point cause an abrupt change in the μ_T profile. To avoid this problem, a smooth function is used to transition from one set of constants to the other set. This works until the outer jet core is about to disappear and the shear layers are about to start merging together. At that point, the mixing length model must be altered and the normal and the inverted velocity profile cases treated separately.

The normal velocity profile mixing length model was developed by observing the behavior of the u and $\partial u/\partial r$ profiles as the shear layers merged in the measured data taken by Lau.[15] A single characteristic length scale for the merging shear layers is defined as

$$\ell = \frac{\Delta U_{\max}}{|\partial u/\partial r|_{\max}}.\qquad(5)$$

where $\Delta U_{\max}$ is the largest ΔU across the two merging shear layers where the separation point between them is defined by the local minimum in the $|\partial u/\partial r|$ profile. The C_1 and C_2 factors are determined from the edge conditions for $\Delta U_{\max}$. The maximum gradient $|\partial u/\partial r|_{\max}$ is the largest value of $|\partial u/\partial r|$ that occurs in the merging profile. This approach for determining C_1, C_2, and ℓ for a merging normal profile transitions into the appropriate form for the single jet downstream.

When an inverted velocity profile jet starts to merge, a local maximum occurs in the profile yielding $\partial u/\partial r = 0$. This point identifies the separation point between the two shear layers. As long as the inner core exists, the two merging shear layers are treated separately but their constants are added as follows:

$$(C_1 C_2 \ell)_{\text{total}} = (C_1 C_2 \ell)_{\text{inner}} + (C_1 C_2 \ell)_{\text{outer}}.\qquad(6)$$

This increases μ_T across the profile to mimic the increased turbulent action as the inverted profile starts to merge. When the inner core ends, it is assumed that the outer shear layer mixing process dominates the flow. The constants for the model are reduced to $(C_1 C_2 \ell)_{\text{total}} = (C_1 C_2 \ell)_{\text{outer}}$. This later usage of C_1, C_2, and ℓ also transitions into the appropriate form for a single jet. The unrealistic condition that $\mu_T = 0$ at the local maximum is removed by smoothing the $|\partial u/\partial r|$ profile, and hence smoothing μ_T. This and other details of the model are given in Dahl.[14]

2.2 Numerical Method

The numerical method initially follows the stream function approach given by Crawford and Kays.[16] The equations of motion in boundary layer form are transformed into stream function coordinates and become

$$\frac{\partial u}{\partial x} = \frac{\partial}{\partial \Psi}\left[r^2 \rho u \mu_{\text{eff}}\frac{\partial u}{\partial \Psi}\right]\qquad(7)$$

$$\frac{\partial H}{\partial x} = \frac{\partial}{\partial \Psi}\left[r^2 \rho u \frac{\mu_{\text{eff}}}{Pr_{\text{eff}}}\frac{\partial H}{\partial \Psi}\right]$$

$$+ \frac{\partial}{\partial \Psi}\left[r^2 \rho u^2\left(\mu_{\text{eff}} - \frac{\mu_{\text{eff}}}{Pr_{\text{eff}}}\right)\frac{\partial u}{\partial \Psi}\right]\qquad(8)$$

where H is the total mean enthalpy and

$$\mu_{\text{eff}} = \mu + \mu_T\qquad(9)$$

and

$$Pr_{\text{eff}} = \frac{1 + \frac{\mu_T}{\mu}}{\frac{1}{Pr} + \frac{1}{Pr_T}\frac{\mu_T}{\mu}}.\qquad(10)$$
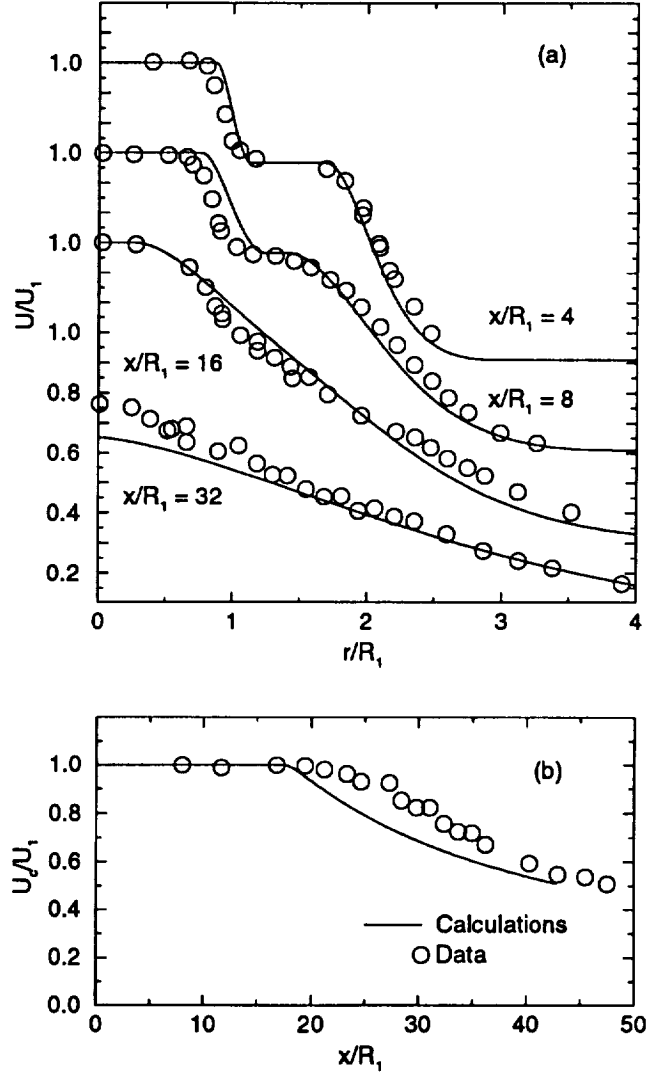

Figure 1: Comparison of NVP predictions with measurements of Lau.[15] (a) radial profiles, staggered scale; (b) centerline velocity

The numerical equations are derived by using fully implicit differencing on equations (7) and (8). This insures that the numerical problem is inherently stable.
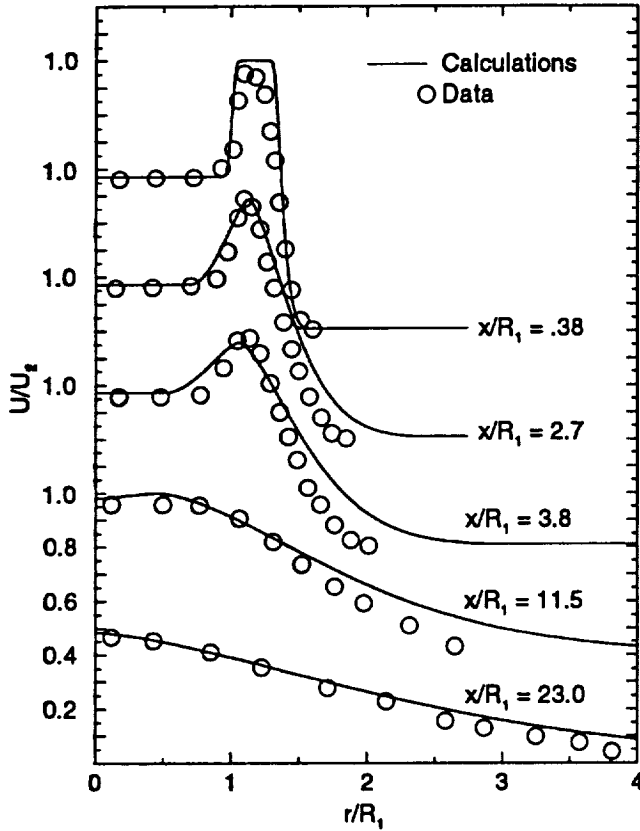
3

Figure 2: Comparison of IVP predictions with measurements of Tanna et al.,[4] radial profiles on staggered scale.

Since both the mean flow and instability wave problems are calculated using the same grid, the required grid resolution is maintained by solving the problems on a fine, evenly spaced r-grid. Details of the finite difference algorithm and solution procedure are given in Dahl.[14]

2.3 Mean Flow Calculations

Figure 1 shows a comparison between calculated normal velocity profiles and measured velocity data from Lau.[15] The operating conditions are: $U_1 = 411$ m/s, $T_1 = 657$ K, $R_1 = 1.96$ cm; $U_2 = 274$ m/s, $T_2 = 292$ K, $R_2 = 3.91$ cm. Initially, the two profiles are very similar. Downstream, deviations increase between calculated and measured profiles and the centerline velocity is underpredicted. This result is indicative of the limitations of the turbulence model. It is only as good as the correlations that were made for shear layer spreading as a function of convected Mach number. Nevertheless, the calculated mean velocity profiles show merging and decay with axial distance in a manner similar to measured data. An example comparison between calculated inverted velocity profiles and measured data[4] is shown in Figure 2. The operating conditions are:

$U_1 = 273$ m/s, $T_1 = 434$ K, $R_1 = 2.61$ cm; $U_2 = 477$ m/s, $T_2 = 758$ K, $R_2 = 3.57$ cm. Again, good agreement is shown in the radial profile comparisons showing that the calculations are capable of producing a reasonable merging jet with an initial inverted velocity profile. In cases where data were available, the mean flow predictions gave good qualitative and often good quantitative resemblance to measured profiles. Thus, we are confident that the prediction scheme describes reasonably the mean flow evolution of coaxial jets. These results are used to calculate the evolution of instability waves and their radiated noise.

3 INSTABILITY WAVES AND RADIATED NOISE

Thin free shear layers that contain an inflection point in the mean velocity profile are inherently unstable even in the absence of viscosity. Initially, an instability wave in the shear layer grows rapidly. As the shear layer grows, the wave growth rate decreases. Eventually, the shear layer is too thick to support unstable waves and the wave amplitude decreases until it disappears. This instability wave process is assumed to be governed by the linearized, inviscid, compressible equations of motion.

For slowly diverging jet flows, two solutions are created that apply to separate but overlapping regions. Following the approach of Tam and Burton,[11] the inner region, including the jet flow and the immediate region just outside the jet, has different length scales in the radial and the axial directions that leads to a multiple scales expansion of the governing equations. With the pressure disturbances represented as

$$p'(r, \theta, x, t) = \sum_{m=0}^{\infty} \delta_m(\varepsilon) p_m(r, s)$$
$$\times \exp\left[i\left(\frac{\phi(s)}{\varepsilon} + n\theta - \omega t\right)\right], \quad (11)$$

the lowest order set of equations in nondimensional form may be reduced to

$$\frac{\partial^2 p_0}{\partial r^2} + \left[\frac{1}{r} + \frac{2\alpha}{\omega - \alpha\bar{u}}\frac{\partial\bar{u}}{\partial r} - \frac{1}{\bar{\rho}}\frac{\partial\bar{\rho}}{\partial r}\right]\frac{\partial p_0}{\partial r}$$
$$+ \left[\bar{\rho}M_j^2(\omega - \alpha\bar{u})^2 - \frac{n^2}{r^2} - \alpha^2\right]p_0 = 0 \quad (12)$$

which is known as the compressible Rayleigh Equation. In equation (11), $\delta_m(\varepsilon)$ are the gauge functions of the asymptotic expansion in the small parameter ε where $\delta_0(\varepsilon) = 1$, s is the slow variable to recognize the slow mean flow development in the axial direction $s = \varepsilon x$, $\phi(s)$ is an axial phase function related to the axial wavenumber α by $d\phi/ds = \alpha(s)$, n is the azimuthal mode number, and ω is the radian frequency.

In the outer region, which slightly overlaps the inner region, the governing equations control disturbances

that are acoustic in nature. These disturbances have the same length scales in all directions; hence, all coordinates are treated equally. To create an outer solution in a form that allows it to be asymptotically matched to the inner solution, we use the axial coordinate $s = \epsilon x$ and the radial coordinate $\bar{r} = \epsilon r$. The solution is obtained by Fourier transforming the outer region governing equations in the s direction. After considerable algebra, the lowest order outer solution is

$$p(r, \theta, x, t) = \int_{-\infty}^{\infty} g(\eta) H_n^{(1)}(i\lambda(\eta)r)e^{i\eta x}e^{in\theta}e^{-i\omega t}d\eta \quad (13)$$

where

$$g(\eta) = \frac{1}{2\pi} \int_{-\infty}^{\infty} \tilde{A}_0(\epsilon x)e^{i\phi(\epsilon x)/\epsilon}e^{-i\eta x}dx \quad (14)$$

and

$$\lambda(\eta) = \left[\eta^2 - \bar{p}_\infty M_j^2(\omega - \eta\bar{u}_\infty)^2\right]^{1/2}. \quad (15)$$

$H_n^{(1)}$ is an nth-order Hankel function of the first kind.

After the inner and the outer solutions are matched asymptotically in an overlap region, we find that equation (12) has become an eigenvalue problem with solutions only for certain values of the eigenvalue α. We have used a finite-difference approximation to discretize the problem. The eigenvalue is found from the resulting diagonal matrix using a Newton-Raphson iteration for refinement.

Since the rate of spread of the jet is slow for high speed jets and ϵ is very small, $\tilde{A}_0(\epsilon x)$ in equation (14) is taken to be constant. Furthermore with $\alpha(x)$ found from the solution of equation (12) at every axial location, the axial phase function is found from $\phi(\epsilon x)/\epsilon = \int_0^x \alpha(\xi)\,d\xi$. We can then solve for $g(\eta)$ in equation (14), the Fourier transform of the instability wave, and subsequently the near field pressure disturbance is found from equation (13). To obtain the pressure in the far field, equation (13), in spherical coordinates, is approximated by the method of stationary phase. The resulting sound power radiated per unit solid angle is

$$D(\psi) = \frac{1}{2}|p|^2R^2 = 2\frac{|g(\bar{\eta})|^2}{\left[1 - M_\infty^2 \sin^2\psi\right]}. \quad (16)$$

The stationary point is given by

$$\bar{\eta} = \frac{\bar{p}_\infty^{1/2}M_j\omega\cos\psi}{(1 - M_\infty^2)\left(1 - M_\infty^2\sin^2\psi\right)^{1/2}} - \frac{\bar{p}_\infty M_j^2\bar{u}_\infty\omega}{1 - M_\infty^2} \quad (17)$$

and ψ is the polar angle.

To validate the mean flow and noise radiation prediction schemes, Dahl and Morris[8] compared calculated results using numerically generated mean flow profiles to

measured data (Seiner and Ponton[17]) and found favorable comparisons in the far field radiated noise patterns even though the numerically generated mean flows had longer potential core lengths than the measured data. However, the calculated initial spreading of the jet was similar to measured data and encompassed the region of maximum growth of the instability wave. Dahl[14] gave further qualitative comparisons with measured coaxial jet data from Tanna et al.[7] and showed that the calculated single frequency far field directivities agreed with the basic trends shown in the measured data. Thus, we assume that given the jet operating conditions, we can calculate the initial jet spreading with sufficient accuracy to obtain reasonable results from the instability wave noise radiation analysis.

4 COAXIAL JET NOISE PREDICTIONS

The mean flow prediction scheme and the instability wave noise generation model are used to conduct a study to gauge the effectiveness of changing various operating parameters on noise generation from coaxial jets. A single jet with exit velocity 1330 m/s and exit temperature 1100 K is chosen as the reference jet. Operating conditions for the coaxial jets are then chosen to have the same total thrust, total mass flow, and total exit area as the reference jet. For both NVP and IVP coaxial jets, we first consider the effects of various velocity and density ratios on noise radiation with the exit area ratio fixed. Next, the area ratio is varied. Finally, the effects of simulated enhanced mixing is considered for both types of coaxial jet velocity profiles.

4.1 Normal Profile Jets

With the area ratio $AR = 1.25$, the mean flow for NVP jets is calculated using the operating conditions given in Table 1. As described in Dahl,[14] the inner potential core length increases with increasing velocity and with decreasing temperature resulting in lower spreading rates for the inner shear layer. The results for the outer potential core length and outer shear layer spreading rate follow a similar pattern. Predictions are then made of the instability wave growth and decay for each shear layer. Using the wavenumber spectrum, eq. (14), the far field radiated noise patterns are calculated from eq. (16). A survey of the noise patterns indicated that the helical, $n = 1$, mode was dominant. Results are shown in Figure 3 for a Strouhal number of 0.2. Only the levels for the instability wave that generates the highest far field levels are included. This could be an instability wave associated with either the inner or the outer shear layer. The four peaks at smaller angles are associated with the outer shear layer instability wave and the four peaks at larger angles are associated with the inner shear layer instability. At this Strouhal number, it appears that the shear layer with the dominant instability wave has the largest ΔU across it. But, we also find that promoting a decrease in the density ratio across

5

a shear layer also promotes instability wave growth and higher radiated noise patterns. Thus, we find conditions where the radiated noise from the inner shear layer has a higher amplitude than the reference jet. The far field noise radiation patterns at other Strouhal numbers have higher or lower peak levels than those shown in Figure 3
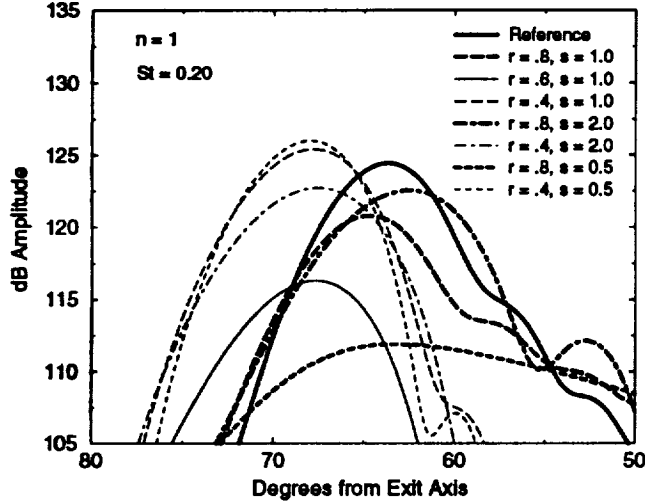

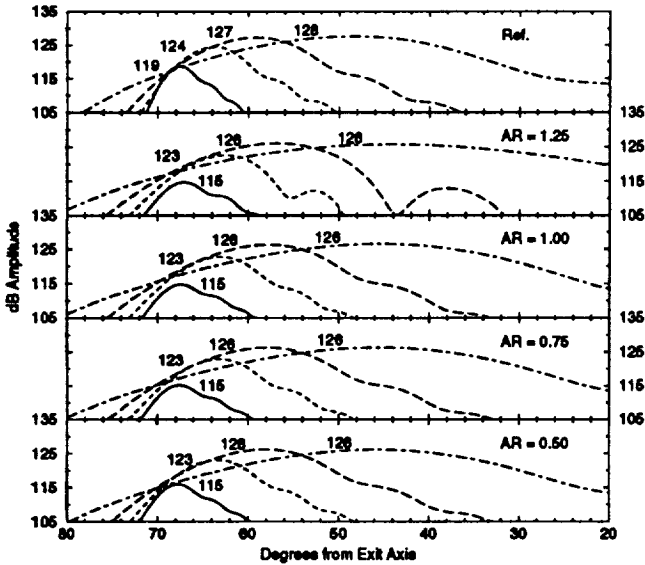Figure 3: Far field directivity patterns for NVP jets for $AR = 1.25$, $n = 1$, $St = .20$

Figure 4: Far field directivity patterns for NVP jets with varying area ratio, $r = .8$, $s = 2$, $n = 1$, outer shear layer. See Figure 5 for legend.

depending on the operating conditions. Examples that illustrate this are shown next. These examples also include the added effect of changing the area ratio.
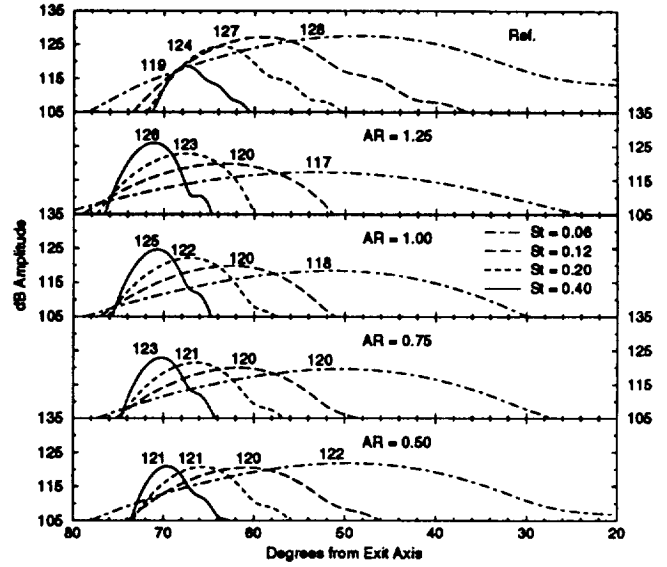

Figure 5: Far field directivity patterns for NVP jets with varying area ratio, $r = .4$, $s = 2$, $n = 1$, inner shear layer.

The general effect of decreasing the area ratio on the mean flow is to decrease the length of the outer potential core and to cause the two shear layers to merge faster. This would then affect the growth and decay of the instability waves and the resulting radiated noise. Two examples of the effects of area ratio changes on radiated noise are shown in Figures 4 and 5. Each figure shows the relative amplitudes of the far field noise radiation patterns associated with four Strouhal numbers with the peak levels labeled on the figures. For a velocity ratio $r = U_2/U_1$ of 0.8, Figure 4 shows that changing the area ratio has little impact on the relative levels of radiated noise from the instability waves in the outer shear layer. The velocity difference across the outer shear layer is much larger than that across the inner shear layer and the radiated noise from the outer shear layer instability waves dominates in the far field. The instability waves in the outer shear layer are not significantly affected by merging the smaller inner shear layer sooner with the much larger outer shear layer.

In contrast, Figure 5 shows what happens when the two shear layers have similar velocity differences. Here, the velocity ratio is 0.4 making the inner shear layer velocity difference slightly larger than the outer shear layer velocity difference resulting in the inner shear layer instability wave dominating the outer shear layer instability wave. As the area ratio decreases, the lower Strouhal number far field amplitudes increase while the higher Strouhal number amplitudes decrease. The reason for this is shown in Figure 6. At Strouhal number 0.4, the local growth rate of the inner shear layer instability wave decreases faster as the shear layers merge sooner with

6

decreasing area ratio. The larger downstream merging shear layer is unable to continue supporting this shorter wavelength instability wave and its growth rate slows and it begins to decay sooner. In contrast, the growth rates for the longer wavelength, lower Strouhal number 0.06 case are enhanced by the earlier merging of the two shear layers. The instability wave grows to a higher amplitude before it begins to decay; a process that is governed by the single fully merged jet downstream.
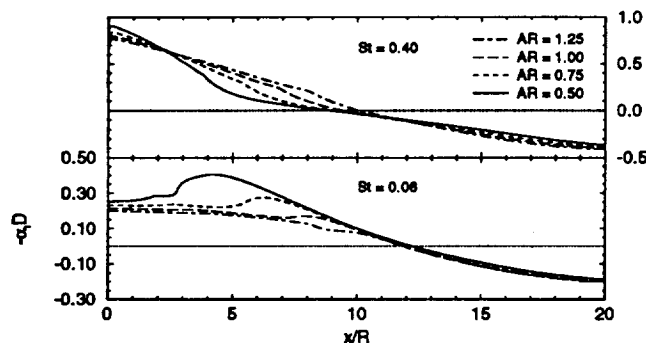

Figure 6: Instability wave local growth rates for NVP jets with varying area ratio, $r = .4$, $s = 2$, $n = 1$, inner shear layer.

4.2 Inverted Profile Jets

In a previous study, Dahl and Morris[8] limited their calculations to IVP jets operated at the minimum noise condition for shock associated noise. This constraint resulted in fixing the density ratio for any given velocity
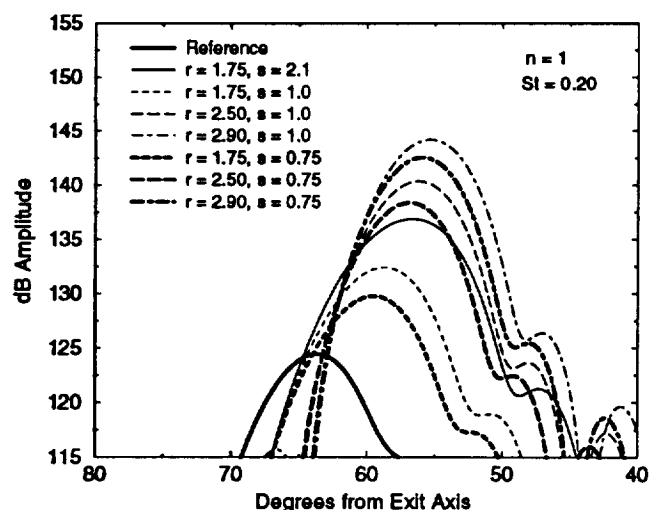

Figure 7: Far field directivity patterns for IVP jets for $AR = 1.25$, $n = 1$, $St = .20$

ratio and area ratio. Here, we remove that constraint and assume for a perfectly expanded jet that we can

vary the density ratio independently of the other operating conditions. However, the thrust, mass flow, and exit area are still held constant as before. Figure 7 shows examples of far field radiated noise patterns generated by the dominant outer shear layer, $n = 1$, helical instability wave for seven IVP jets. Their operating conditions are given in Table 1. The trends of the relative changes for the Strouhal number 0.2 results are representative of results at other frequencies. The plots show that radiated noise increases with larger r due to a higher velocity in the outer stream relative to ambient. Also, the plots show that heating the outer stream, $s < 1$, reduces the relative level of radiated noise since heating reduces the growth of the outer shear layer instability wave.
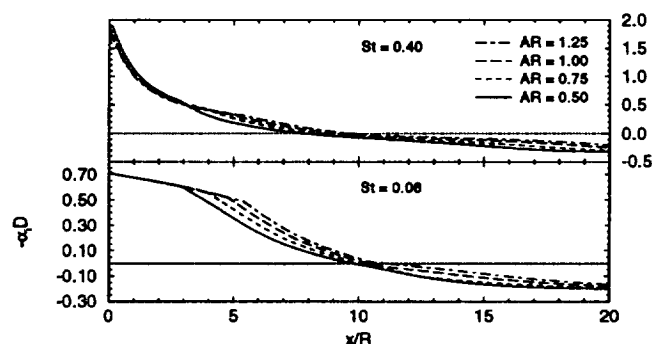

Figure 8: Instability wave local growth rates for IVP jets with varying area ratio, $r = 1.75$, $s = .75$, $n = 1$, outer shear layer.
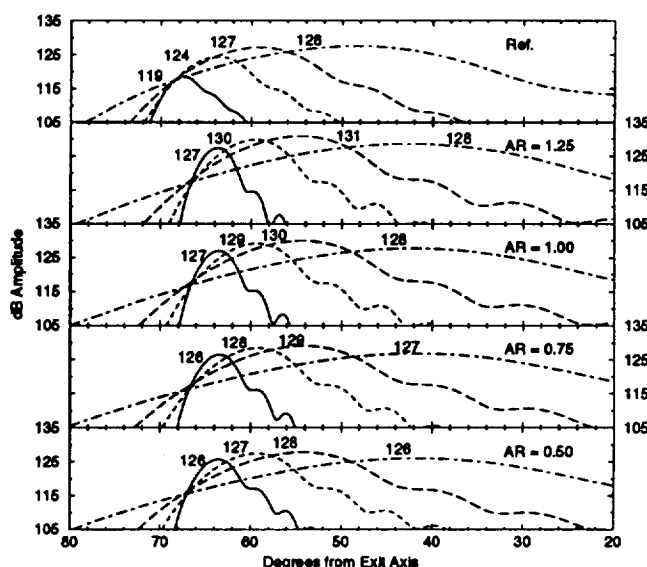

Figure 9: Far field directivity patterns for IVP jets with varying area ratio, $r = 1.75$, $s = .75$, $n = 1$, outer shear layer. See Figure 5 for legend.
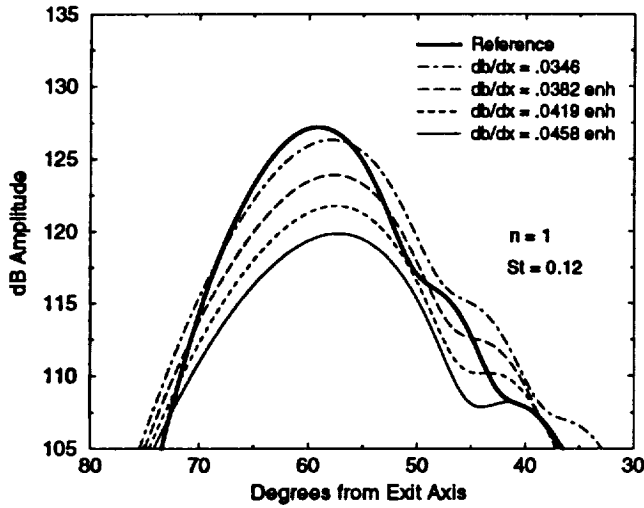
7

Figure 10: Effects of enhanced mixing on radiated noise from NVP jets, $r = .8$, $s = 2$, $AR = .75$, outer shear layer.

Figure 11: Effects of enhanced mixing on radiated noise from IVP jets, $r = 1.75$, $s = .75$, $AR = .75$, outer shear layer.

As with the NVP jets, decreasing the area ratio of an IVP jet decreases the length of the outer potential core even though the outer stream velocity must increase to maintain constant thrust and mass flow. With the two shear layers merging sooner, the instability wave growth rates in the outer shear layer are diminished sooner as seen in Figure 8. For both Strouhal number 0.06 and 0.4 instability waves, the local growth rates decrease more rapidly after the end of the outer potential core and the instability waves become damped sooner as the merging mean flow spreads. The resulting far field noise radiation patterns are shown in Figure 9. The relative peak levels are decreasing with a smaller area ratio, with more reduction at lower Strouhal numbers than at higher Strouhal numbers. Note that relative to the single reference jet, the higher Strouhal number patterns for the IVP jet have higher relative levels than the lower Strouhal number patterns. This trend was observed by Tanna[18] where shock free IVP jets were noisier than the single reference jet at high frequencies and quieter at low frequencies.

4.3 Effects of Enhanced Mixing

Recently, Dahl and Morris[19] studied the effects of simulated enhanced mixing on the instability wave noise generation process in single, supersonic jets. The simulation of enhanced mixing in the mean flow was accomplished by multiplying equation (3) by an additional constant greater than one to increase μ_T across the shear layer. For coaxial jets using the current model, this results in enhancing both shear layers.

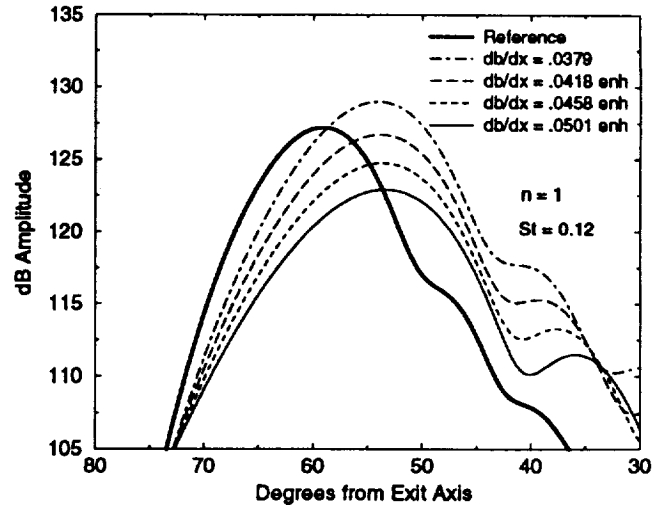With both shear layers growing faster with enhancement and the potential core lengths shortening, the instability waves that grow in the shear layers, grow to lower total amplitudes. Assuming the initial instability wave amplitude remains unchanged during enhancement, this results in a lower level of far field radiated noise from the enhanced jet than from the non-enhanced jet. An example of the effects of enhancement on the radiated noise from an NVP jet is shown in Figure 10. The velocity ratio is 0.8 and the inner stream is twice as hot as the outer stream. Thus, the dominant noise is generated in the outer shear layer. The degree of spreading is determined by the rate of change in the initial shear layer half-width b in the core region. For an initial 10% increase in spreading rate, the figure shows about a 2.5 dB decrease in peak levels at Strouhal number 0.12. Further increases in spreading rate lead to further reductions in peak level; but, the amount of reduction is decreasing as the level of enhancement increases. A similar result is seen in Figure 11 for an IVP jet with velocity ratio 1.75 and a hot outer stream.

5 DISCUSSION

The results shown in this paper for coaxial jets are based on the relative changes that occur compared to a single reference jet where total thrust, mass flow, and exit area are held constant. With the operating conditions fixed for the Mach 2 reference jet, we have explored only a part of the operating conditions that are possible for coaxial jets. Furthermore, without knowing the initial amplitudes of the instability waves, it is difficult to specify which operating conditions will actually lead to less far field radiated noise compared to other operating conditions. Thus, we are currently left to consider the relative trends that are shown in the calculated results.

For both NVP and IVP jets, there are relative noise reduction benefits when operating the coaxial jets with

8

velocity ratios closer to 1 than further from 1. From a practical standpoint, there are benefits for operating with the higher velocity stream hotter than the lower velocity stream. This is especially beneficial in the IVP jet case.

When the effects of area ratio changes are included, we find for the NVP jets with velocity ratios near 1 that no significant changes occur in the instability wave growth that effect the far field radiated noise levels. For IVP jets, the effects of area ratio reductions are to reduce the growth of the instability waves leading to less radiated noise. However, the IVP jet promotes high frequency noise relative to the single reference jet.

The effects of simulated enhanced mixing on reducing radiated noise were modest compared to the relative effects of operating condition changes. But, regardless of the operating condition, mixing enhancement was a means to further reduce relative far field radiated noise levels.

REFERENCES

1. J. M. Seiner and E. A. Krejsa. Supersonic Jet Noise and the High Speed Civil Transport. Paper No. 89-2358, AIAA, 1989.

2. J. C. Yu and D. S. Dosanjh. Noise Field of Coaxial Interacting Supersonic Jet Flows. Paper No. 71-152, AIAA, 1971.

3. H. K. Tanna, W. H. Brown, and C. K. W. Tam. Shock Associated Noise of Inverted-profile Coannular Jets, Part I: Experiments. *J. Sound Vib.*, 98:95–113, 1985.

4. H. K. Tanna, B. J. Tester, and J. C. Lau. The Noise and Flow Characteristics of Inverted-Profile Coannular Jets. CR-158995, NASA, 1979.

5. H. K. Tanna and P. J. Morris. The Noise from Normal-Velocity-Profile Coannular Jets. *J. Sound Vib.*, 98:213–234, 1985.

6. H. K. Tanna. An Experimental Study of Jet Noise, Part II: Shock Associated Noise. *J. Sound Vib.*, 50:429–444, 1977.

7. H. K. Tanna, W. H. Brown, and C. K. W. Tam. Shock Associated Noise Reduction from Inverted Velocity Profile Coannular Jets. CR-3454, NASA, 1981.

8. M. D. Dahl and P. J. Morris. Noise Radiation by Instability Waves in Coaxial Jets. Paper No. 94-2190, AIAA, 1994.

9. K. K. Ahuja. Mixing Enhancement and Jet Noise Reduction Through Tabs Plus Ejectors. Paper No. 93-4347, AIAA, 1993.

10. A. Michalke. Survey of Jet Instability Theory. *Prog. Aerospace Sci.*, 21:159–199, 1984.

11. C. K. W. Tam and D. E. Burton. Sound Generated by Instability Waves of Supersonic Flows. Part 2. Axisymmetric Jets. *J. Fluid Mech.*, 138:273–295, 1984.

12. P. J. Morris. A Model for Broadband Jet Noise Amplification. Paper No. 80-1004, AIAA, 1980.

13. P. J. Morris and C. Baltas. Turbulence in Sound Excited Jets: Measurements and Theory. Paper No. 81-0058, AIAA, 1981.

14. M. D. Dahl. *The Aeroacoustics of Supersonic Coaxial Jets*. PhD thesis, Penn State University, 1994.

15. J. C. Lau. A Study of the Structure of the Coannular Jet. LG80ER0017, Lockheed-Georgia Co., 1980.

16. M. E. Crawford and W. M. Kays. Stan5 - A Program for Numerical Computation of Two Dimensional Internal and External Boundary Layer Flows. CR-2742, NASA, 1976.

17. J. M. Seiner and M. K. Ponton. Aeroacoustic Data for High Reynolds Number Supersonic Axisymmetric Jets. TM-86296, NASA, 1985.

18. H. K. Tanna. Coannular Jets – Are They Really Quiet and Why? *J. Sound Vib.*, 72:97–118, 1980.

19. M. D. Dahl and P. J. Morris. Supersonic Jet Noise Reductions Predicted with Increased Jet Spreading Rate. TM-106872, NASA, 1995.

AR	r	s	U1(m/s)	U2(m/s)	T1(K)	T2(K)	M1	M2
Reference Jet								
–	–	–	1330.0	–	1100.0	–	2.0	–
NVP Jets								
1.25	0.80	1.00	1477.8	1182.2	1086.4	1086.4	2.2	1.8
1.25	0.60	1.00	1605.2	963.1	1032.6	1032.6	2.5	1.5
1.25	0.40	1.00	1662.2	665.0	916.7	916.7	2.7	1.1
1.25	0.80	2.00	1534.6	1227.7	1692.3	846.2	1.9	2.1
1.25	0.40	2.00	1900.0	760.0	1396.8	698.4	2.5	1.4
1.25	0.80	0.50	1425.0	1140.0	785.7	1571.4	2.5	1.4
1.25	0.40	0.50	1511.4	604.5	694.4	1388.9	2.9	0.8
1.00	0.80	2.00	1516.7	1213.3	1630.7	815.3	1.9	2.1
0.75	0.80	2.00	1492.8	1194.3	1552.2	776.1	1.9	2.1
0.50	0.80	2.00	1459.7	1167.8	1448.8	724.4	1.9	2.2
1.00	0.40	2.00	1813.6	725.5	1350.0	675.0	2.5	1.4
0.75	0.40	2.00	1716.1	686.5	1297.7	648.8	2.4	1.3
0.50	0.40	2.00	1605.2	642.1	1239.1	619.5	2.3	1.3
IVP Jets								
1.25	1.75	2.10	823.7	1441.4	1678.4	808.1	1.0	2.5
1.25	1.75	1.00	878.1	1536.6	1028.8	1028.8	1.4	2.4
1.25	2.50	1.00	622.6	1556.4	943.9	943.9	1.0	2.5
1.25	2.90	1.00	534.3	1549.5	908.4	908.4	0.9	2.6
1.25	1.75	0.75	907.2	1587.7	880.6	1174.2	1.5	2.3
1.25	2.50	0.75	648.3	1620.8	796.9	1062.5	1.2	2.5
1.25	2.90	0.75	556.7	1614.4	761.0	1014.6	1.0	2.5
1.00	1.75	0.75	932.9	1632.6	892.1	1189.5	1.6	2.4
0.75	1.75	0.75	969.3	1696.4	909.1	1212.1	1.6	2.4
0.50	1.75	0.75	1025.3	1794.3	936.3	1248.4	1.7	2.5

Area Ratio $AR = A2/A1$

Velocity Ratio $r = U2/U1$ Density Ratio $s = \rho2/\rho1 = T1/T2$

(Constant Thrust and Constant Mass Flow)

Table 1: Operating Conditions for Supersonic Coaxial Jet Calculations.

REPORT DOCUMENTATION PAGE

Public reporting burden for this collection of information is estimated to average 1 hour per response, including the time for reviewing instructions, searching existing data sources, gathering and maintaining the data needed, and completing and reviewing the collection of information. Send comments regarding this burden estimate or any other aspect of this collection of information, including suggestions for reducing this burden, to Washington Headquarters Services, Directorate for Information Operations and Reports, 1215 Jefferson Davis Highway, Suite 1204, Arlington, VA 22202-4302, and to the Office of Management and Budget, Paperwork Reduction Project (0704-0188), Washington, DC 20503.

1. AGENCY USE ONLY (Leave blank)	2. REPORT DATE	3. REPORT TYPE AND DATES COVERED
	May 1995	Technical Memorandum

4. TITLE AND SUBTITLE

Supersonic Coaxial Jet Noise Predictions

5. FUNDING NUMBERS

WU–505–62–52

6. AUTHOR(S)

Milo D. Dahl and Philip J. Morris

7. PERFORMING ORGANIZATION NAME(S) AND ADDRESS(ES)

National Aeronautics and Space Administration
Lewis Research Center
Cleveland, Ohio 44135–3191

8. PERFORMING ORGANIZATION REPORT NUMBER

E–9584

9. SPONSORING/MONITORING AGENCY NAME(S) AND ADDRESS(ES)

National Aeronautics and Space Administration
Washington, D.C. 20546–0001

10. SPONSORING/MONITORING AGENCY REPORT NUMBER

NASA TM–106917
CEAS/AIAA–95–171

11. SUPPLEMENTARY NOTES

Prepared for the First Joint Aeroacoustics Conference cosponsored by Confederation of European Aerospace Societies and the American Institute of Aeronautics and Astronautics, Munich, Germany, June 12–15, 1995. Milo D. Dahl, NASA Lewis Research Center, and Philip J. Morris, Pennsylvania State University, University Park, Pennsylvania 16802. Responsible person, Milo D. Dahl, organization code 2660, (216) 433–3578.

12a. DISTRIBUTION/AVAILABILITY STATEMENT

Unclassified - Unlimited
Subject Category 71

This publication is available from the NASA Center for Aerospace Information, (301) 621–0390.

12b. DISTRIBUTION CODE

13. ABSTRACT (Maximum 200 words)

Predictions are made for the noise radiation from supersonic, coaxial jets. These predictions are based on the assumption that the noise radiation in the downstream direction of supersonic jets is dominated by sound generated by instability waves with supersonic phase velocities relative to ambient. Since the analysis requires a known mean flow and the coaxial jet mean flow is not described easily in terms of analytic functions, a numerical prediction is made for its development. The compressible, Reynolds averaged, boundary layer equations are solved with a modified mixing length turbulence model. The model has been calibrated to account for compressibility and temperature effects on the rate of mixing. Both normal and inverted velocity profile jets are considered. Predictions are made for the differences between the noise radiated by coaxial jets with different operating conditions and a single reference jet with the same thrust, mass flow, and exit area. The effects of area ratio changes and simulated enhanced mixing on noise radiation are also considered.

14. SUBJECT TERMS

Supersonic coaxial jets; Noise radiation; Instability waves; Mean flow prediction; Noise prediction; Noise reduction

15. NUMBER OF PAGES

12

16. PRICE CODE

A03

17. SECURITY CLASSIFICATION OF REPORT	18. SECURITY CLASSIFICATION OF THIS PAGE	19. SECURITY CLASSIFICATION OF ABSTRACT	20. LIMITATION OF ABSTRACT
Unclassified	Unclassified	Unclassified	

NSN 7540-01-280-5500

Standard Form 298 (Rev. 2-89)
Prescribed by ANSI Std. Z39-18
298-102